



Stratospheric water vapor: an important climate feedback

Antara Banerjee^{1,2,3} · Gabriel Chiodo¹ · Michael Previdi⁴ · Michael Ponater⁵ · Andrew J. Conley⁶ · Lorenzo M. Polvani¹

Received: 20 July 2018 / Accepted: 8 March 2019 / Published online: 1 April 2019
© Springer-Verlag GmbH Germany, part of Springer Nature 2019

Abstract

The role of stratospheric water vapor (SWV) changes, in response to increasing CO₂, as a feedback component of quantitative significance for climate sensitivity has remained controversial. Here, we calculate the SWV climate feedback under abrupt CO₂ quadrupling in the CMIP5 ensemble of models. All models robustly show a moistening of the stratosphere, causing a global mean net stratosphere adjusted radiative perturbation of $0.89 \pm 0.27 \text{ Wm}^{-2}$ at the reference tropopause. The stratospheric temperature adjustment is a crucial component of this radiative perturbation. The associated climate feedback is $0.17 \pm 0.05 \text{ Wm}^{-2} \text{ K}^{-1}$, with a considerable inter-model range of $0.12\text{--}0.28 \text{ Wm}^{-2} \text{ K}^{-1}$. Taking into account the rise in tropopause height under $4 \times \text{CO}_2$ slightly reduces the feedback to $0.15 \pm 0.04 \text{ Wm}^{-2} \text{ K}^{-1}$, with a range of $0.10\text{--}0.26 \text{ Wm}^{-2} \text{ K}^{-1}$. The SWV radiative perturbation peaks in the midlatitudes and not the tropics: this is due primarily to increases in SWV in the extratropical lowermost stratosphere, which cause the majority (over three quarters) of the global mean feedback. Based on these results, we suggest an increased focus on understanding drivers of water vapor trends in the extratropical lowermost stratosphere. We conclude that the SWV feedback is important, being on the same order of magnitude as the global mean surface albedo and cloud feedbacks in the multi-model mean.

Keywords Stratospheric water vapor · Climate feedback · Climate change · Partial radiative perturbation · Radiative kernel · CMIP5 models

Electronic supplementary material The online version of this article (<https://doi.org/10.1007/s00382-019-04721-4>) contains supplementary material, which is available to authorized users.

✉ Antara Banerjee
antara.banerjee@noaa.gov

- ¹ Department of Applied Physics and Applied Mathematics, Columbia University, New York, NY, USA
- ² Present Address: Cooperative Institute for Research in Environmental Sciences, University of Colorado Boulder, Boulder, CO, USA
- ³ Present Address: National Oceanic and Atmospheric Administration/Earth System Research Laboratory/Chemical Sciences Division, Boulder, CO, USA
- ⁴ Department of Earth and Environmental Sciences, Lamont Doherty Earth Observatory, Palisades, New York, NY, USA
- ⁵ Deutsches Zentrum für Luft- und Raumfahrt (DLR), Institut für Physik der Atmosphäre, Oberpfaffenhofen, 82230 Weßling, Germany
- ⁶ National Center for Atmospheric Research, Boulder, Colorado, USA

1 Introduction

The overall sensitivity of the climate system to increases in CO₂ depends upon feedbacks that either amplify or diminish the initial forced warming. The traditional set of feedbacks commonly considered comprises changes in temperature (sometimes separated into Planck and lapse rate components), water vapor, surface albedo and clouds; a wealth of studies have focused on quantifying these feedbacks and understanding their inter-model ranges (e.g. Bony et al. 2006; Soden et al. 2008; Vial et al. 2013; Chung and Soden 2015). Specific among this large body of literature are a few studies that have singled out stratospheric water vapor (SWV) as a potential positive climate feedback. We first discuss these studies in detail to contextualize the present work.

Forster and Shine (2002) placed an early upper limit on the SWV climate feedback of around $1.5 \text{ Wm}^{-2} \text{ K}^{-1}$, based on the limited observations available at the time, but acknowledged that these observations could simply reflect decadal variability rather than a long-term trend. Indeed, although interannual variations in SWV, and their associated

Table 1 SWV-driven radiative perturbations (Wm^{-2}) at the tropopause and the associated climate feedbacks ($\text{Wm}^{-2} \text{K}^{-1}$). The stratosphere and troposphere are separated using the piControl tropopause definition. The final column shows the surface temperature change (K) due to $4 \times \text{CO}_2$

Model	Instantaneous, tropopause				Adjusted, tropopause				ΔT_s
	LW	SW	Net	Feedback	LW	SW	Net	Feedback	
ACCESS1-0	1.69	-0.27	1.42	0.26	1.31	-0.28	1.03	0.18	5.56
ACCESS1-3	1.25	-0.19	1.06	0.22	0.92	-0.20	0.72	0.15	4.86
bcc-csm1-1-m	1.39	-0.22	1.17	0.23	1.05	-0.23	0.82	0.16	5.03
bcc-csm1-1	1.06	-0.17	0.89	0.19	0.80	-0.18	0.63	0.13	4.81
BNU-ESM	1.55	-0.25	1.30	0.21	1.17	-0.26	0.91	0.15	6.21
CanESM2	1.46	-0.21	1.24	0.21	1.06	-0.23	0.83	0.14	5.83
CCSM4	0.99	-0.16	0.83	0.17	0.78	-0.17	0.62	0.13	4.78
CNRM-CM5	1.63	-0.26	1.37	0.26	1.27	-0.27	0.99	0.19	5.23
CNRM-CM5-2	1.67	-0.27	1.40	0.27	1.30	-0.28	1.02	0.20	5.20
CSIRO-Mk3-6-0	2.68	-0.44	2.24	0.40	2.00	-0.46	1.55	0.28	5.55
FGOALS-g2	1.00	-0.16	0.84	0.17	0.75	-0.16	0.59	0.12	4.96
FGOALS-s2	1.36	-0.20	1.16	0.20	1.02	-0.21	0.80	0.14	5.77
GFDL-CM3	1.83	-0.29	1.54	0.27	1.35	-0.30	1.06	0.18	5.79
GFDL-ESM2G	1.58	-0.25	1.33	0.36	1.19	-0.25	0.94	0.25	3.71
GFDL-ESM2M	1.69	-0.26	1.43	0.37	1.27	-0.27	1.00	0.26	3.83
GISS-E2-H	0.89	-0.13	0.77	0.19	0.64	-0.13	0.51	0.13	4.05
GISS-E2-R	0.84	-0.12	0.72	0.21	0.60	-0.12	0.48	0.14	3.39
HadGEM2-ES	1.71	-0.25	1.46	0.23	1.25	-0.26	0.99	0.16	6.24
IPSL-CM5A-MR	2.60	-0.41	2.19	0.38	1.92	-0.42	1.50	0.26	5.77
IPSL-CM5B-LR	1.25	-0.18	1.07	0.25	0.92	-0.19	0.74	0.17	4.35
MIROC5	0.96	-0.15	0.81	0.19	0.73	-0.15	0.57	0.14	4.18
MIROC-ESM	1.81	-0.29	1.52	0.23	1.36	-0.30	1.06	0.16	6.62
MPI-ESM-LR	1.94	-0.31	1.63	0.28	1.45	-0.32	1.13	0.19	5.89
MPI-ESM-MR	1.74	-0.27	1.47	0.26	1.30	-0.28	1.01	0.18	5.64
MPI-ESM-P	1.91	-0.30	1.60	0.28	1.42	-0.32	1.11	0.19	5.70
MRI-CGCM3	1.56	-0.25	1.30	0.30	1.18	-0.26	0.91	0.21	4.35
NorESM1-M	0.81	-0.13	0.68	0.16	0.61	-0.13	0.48	0.12	4.14
Mean	1.51	-0.24	1.28	0.25	1.13	-0.25	0.89	0.17	5.09
Std. dev.	0.47	0.08	0.40	0.07	0.35	0.08	0.27	0.05	0.86
Min.	0.81	-0.44	0.68	0.16	0.60	-0.46	0.48	0.12	3.39
Max.	2.68	-0.12	2.24	0.40	2.00	-0.12	1.55	0.28	6.62

climate impacts, can be large (Solomon et al. 2010; Gilford et al. 2016), satellite datasets indicate no long term trend in SWV (at least in the lower stratosphere) in recent decades (Hegglin et al. 2014; Dessler et al. 2014). However, the possibility of a substantial long-term feedback remains, since climate models robustly project increasing SWV with increasing CO_2 (Gettelman et al. 2010; Smalley et al. 2017). Stuber et al. (2001a) simulated the SWV response to a CO_2 perturbation (equivalent to 1 Wm^{-2}) using a single model (ECHAM4). They calculated an associated stratosphere adjusted radiative perturbation at the tropopause of 0.193 Wm^{-2} , which would imply a climate feedback of $0.24 \text{ Wm}^{-2} \text{K}^{-1}$ (calculated from their Table 1). Similarly, and more recently, Dessler et al. (2013) simulated the SWV response over the period 2000–2100 under the A1B greenhouse gas emissions scenario, again using a single model (GEOSCCM). They calculated an associated

stratosphere adjusted radiative perturbation at the tropopause of 0.59 Wm^{-2} , which would imply a climate feedback of $0.29 \text{ Wm}^{-2} \text{K}^{-1}$. Finally, in a multi-model study, Huang et al. (2016) calculated the SWV response to abrupt CO_2 quadrupling in an ensemble of the Coupled Model Intercomparison Project (CMIP5) models. They reported a multi-model mean feedback of $0.02 \pm 0.01 \text{ Wm}^{-2} \text{K}^{-1}$ using two instantaneous top-of-the-atmosphere (ToA) radiative kernels (from the NCAR and GFDL models). However, these kernel calculations did not include stratospheric temperature adjustment, which must be accounted for in order to reliably estimate the climate impacts of changing stratospheric constituents (e.g. Forster and Shine 1997; Solomon et al. 2010; Maycock and Shine 2012). In summary, previous literature suggests a likely SWV feedback of around $0.24\text{--}0.29 \text{ Wm}^{-2} \text{K}^{-1}$ (Stuber et al. 2001a; Dessler et al. 2013). We stress, however, that this is based on just two single model studies: these

results remain to be confirmed and the inter-model range needs to be quantified. These are the goals of the present study.

Quantification of the SWV climate feedback has not yet become a routine part of traditional feedback analysis, being either implicitly included within other feedbacks or at least partly excluded. We recall a few examples from the literature. A common technique in diagnosing climate feedbacks is the use of radiative kernels (Soden and Held 2006; Soden et al. 2008), which canonically describe the instantaneous ToA radiative perturbation¹ due to incremental changes in the feedback variable. Several studies integrate kernel-based feedbacks only up to the tropopause (Soden and Held 2006; Soden et al. 2008; Previdi 2010; Vial et al. 2013), with a view to quantify tropospheric feedbacks, thus ostensibly omitting the SWV feedback². The potential importance of including stratospheric contributions is highlighted by Huang (2013). Sanderson et al. (2010) and Klocke et al. (2013) integrate through the full atmospheric column for the water vapor feedback, thereby capturing the portion of the SWV feedback resulting from its *instantaneous* radiative effects. However, the radiative flux change contribution from the stratospheric temperature adjustment is excluded³. Radiative kernels have also been combined with the linear regression approach of Gregory et al. (2004), either integrating up to the tropopause (Liu et al. 2018) or through the full atmospheric column (Block and Mauritsen 2013). The latter method fully captures the SWV feedback: the instantaneous and stratosphere adjusted portions are included within the water vapor and temperature feedbacks, respectively. Another method of calculating climate feedbacks is by Partial Radiative Perturbation (PRP) (Wetherald and Manabe 1988), in which offline calculations determine the radiative effects of individual variables. As with the kernels, some studies (Klocke et al. 2013) capture only the instantaneous portion of the SWV feedback using PRP. Others (Meraner et al. 2013; Colman and McAvaney 2011) combine the PRP and regression methods and thus capture the full SWV feedback as part of the water vapor and temperature feedbacks. Summarizing, we deduce a clear inconsistency among previous studies in their treatment of the SWV feedback and

no clear quantification of its overall effects (instantaneous plus stratosphere adjusted). In the present paper, we provide a multi-model based quantification of the SWV feedback using a standard method to highlight its importance in the context of climate feedback analysis.

In quantifying the SWV feedback, we will distinguish between SWV in the lowermost stratosphere (LMS, between the tropopause and 100 hPa), most of which lies in the extratropics, and the stratospheric overworld (above 100 hPa), owing to their distinct drivers. A primary control on overworld SWV are the cold point temperatures (CPT) in the tropical tropopause layer (TTL), which determine entry mixing ratios into the stratosphere (Holton and Gettelman 2001; Fueglistaler and Haynes 2005). Model studies suggest that increasing CO₂ moistens the overworld by warming the CPT, which results through increases in tropospheric temperatures, offset partially by the effects of a strengthening Brewer-Dobson circulation (Gettelman et al. 2009; Dessler et al. 2013; Smalley et al. 2017). Recent work has identified increases in convectively lofted ice and subsequent evaporation in and above the TTL as another significant contribution to the moistening of the overworld under increasing CO₂ in models (Dessler et al. 2016). In contrast to overworld SWV, there is limited understanding of the processes controlling water vapor variability in the extratropical LMS. Broadly speaking, it is affected by the stratospheric residual circulation, isentropic transport of high water vapor amounts from the tropical troposphere (Dethof et al. 2000; Pan et al. 2000) and possibly from the TTL (Gilford et al. 2016), and by convective moistening (e.g. Sun and Huang 2015). Although the drivers of water vapor in the extratropical LMS have received relatively little attention, it is disproportionately important for the overall stratospheric temperature response and the radiative perturbation from uniform increases in SWV (Solomon et al. 2010; Maycock et al. 2011) and from interannual SWV variations (Gilford et al. 2016). Importantly, Dessler et al. (2013) found that SWV in the LMS is responsible for the majority (two-thirds) of the total SWV climate feedback; this single model result ought to be validated against evidence from a variety of models.

Thus, the goal of this study is to quantify the SWV climate feedback in a *multi-model* framework and determine the inter-model range. To this end, we use the abrupt 4 × CO₂ experiment of the CMIP5 models, which has been widely used to quantify climate feedbacks (e.g. Vial et al. 2013). The SWV climate feedback is calculated with offline radiative transfer calculations, broadly following the PRP methodology, and the effect of the stratospheric temperature adjustment is quantified.

¹ To our knowledge, Solomon et al. (2010) is the only study to include the effects of stratospheric temperature adjustment in their (water vapor) kernel.

² Many of these studies define the tropopause as 100 hPa at the tropics decreasing linearly in latitude to 300 hPa at the poles, so may include some of the lowermost stratosphere in their vertically integrated feedbacks.

³ Here the stratosphere adjusted portion of the SWV feedback is *not* included within the lapse rate feedback, which is integrated only up to the tropopause, in order to exclude fast stratospheric temperature changes associated with CO₂ forcing, as an upgrade upon earlier work (Shell et al. 2008).

2 Models, data and methodology

This study utilises data from 27 CMIP5 models, listed in Table 1. We analyze monthly mean output from the pre-industrial control (piControl) and the abrupt $4 \times \text{CO}_2$ experiment (first ensemble member only), where an instantaneous quadrupling of CO_2 from piControl conditions is imposed at the beginning of the run. The last 50 years of each experiment (out of 150 years for abrupt $4 \times \text{CO}_2$) are analyzed. The zonal and climatological monthly mean of the water vapor fields is calculated for each experiment and model. These fields are interpolated to a common grid ($1.9 \times 2.5^\circ$ horizontal resolution with 26 vertical levels) and input into the offline radiative transfer code, which is now described.

2.1 Calculation of SWV radiative perturbation and feedback

We first calculate the all-sky radiative flux change associated with the SWV response using the Parallel Offline Radiative Transfer (PORT) model (Conley et al. 2013). The methodology broadly follows a Partial Radiative Perturbation (PRP) approach (Wetherald and Manabe 1988), although some differences to the standard procedure will be noted. For each model, a pair of calculations is performed: (i) a reference calculation that uses the model specific piControl water vapor field and (ii) a perturbed calculation that substitutes the abrupt $4 \times \text{CO}_2$ water vapor field. In both these calculations, the water vapor perturbation is applied only in the portion of the atmosphere above the tropopause and below 10 hPa, which is the lowest top in our ensemble of CMIP5 models. The lapse rate tropopause, identified by the lowest level at which the lapse decreases to 2 K km^{-1} (WMO 1957), is used to separate the troposphere and stratosphere across all the models, and is defined using temperatures from piControl conditions within PORT (Conley et al. 2013). Since the tropopause rises in response to tropospheric warming under $4 \times \text{CO}_2$, changing the separation between tropospheric and stratospheric water vapor, the sensitivity of the results to the choice of tropopause is also tested.

The radiative perturbation of the SWV response is measured as the global and annual mean difference in longwave (LW), shortwave (SW) and net (LW+SW) radiative fluxes between the reference and perturbed calculations; we take this difference at both the tropopause and the ToA. Both the instantaneous and stratosphere adjusted radiative perturbations (R_{ins} and R_{adj} , respectively) are calculated. In the latter, stratospheric temperatures are iteratively adjusted above the tropopause to attain radiative

equilibrium using the fixed dynamical heating (FDH) approximation (e.g. Ramanathan and Dickinson 1979; Fels et al. 1980), which is described in the Appendix. We thus calculate four sets of values for each model: R_{ins} and R_{adj} at the tropopause (Table 1) and at the ToA (Supplementary Table 1). For R_{adj} , we calculate two further sets of values using the PORT abrupt $4 \times \text{CO}_2$ tropopause definition (Supplementary Tables 2 and 3). The associated climate feedback is calculated by normalizing net R_{ins} and R_{adj} by the change in global and annual mean surface air temperature due to $4x\text{CO}_2$ (ΔT_s).

Our methodology of calculating the SWV climate feedback is similar to that used by Dessler et al. (2013). It differs from the traditional PRP procedure (Wetherald and Manabe 1988; Colman and McAvaney 1997; Klocke et al. 2013; Colman 2015; Rieger et al. 2017) because we here use a time average of the model output fields (monthly means rather than sub-sampling instantaneous output) and, crucially, because we consider the effect of the stratospheric temperature adjustment. Furthermore, to facilitate a direct comparison with Dessler et al. (2013), we will primarily focus on the radiative feedback calculated at the tropopause rather than the ToA, noting that for net R_{adj} , the values at the tropopause and ToA are almost identical, with no difference in the multi-model mean feedback (compare Table 1 and Supplementary Table 1). Note that we only perform a ‘forward’ PRP-like calculation for each model, in which the abrupt $4 \times \text{CO}_2$ water vapor field is substituted into piControl conditions. For ideal results consistent with a canonical PRP feedback analysis, we would have also needed to perform a ‘backward’ calculation, in which the piControl water vapor field is substituted into abrupt $4 \times \text{CO}_2$ conditions; the average of the forward and backward calculations should provide a better estimate of the SWV feedback (Colman and McAvaney 1997). Given the computational expense, we have only performed this exercise for the Whole Atmosphere Community Climate Model (WACCM) chemistry-climate model (CCM). For this single model, we find that the SWV feedback from the backward calculation is only 0.2% smaller than for the forward calculation, suggesting that it is not critical here to omit the backward calculation.

For comparison with the CMIP study of Huang et al. (2016), we also compute the SWV climate feedback using an instantaneous ToA radiative kernel. We use the same kernel (from the MPI ECHAM5 GCM) and methodology as Previdi (2010) and Previdi and Liepert (2012). Briefly, for each model, we calculate the SWV climate feedback by multiplying the SWV response by the kernel on a 3D monthly mean basis, and normalizing by ΔT_s . Here we separate the stratosphere and troposphere with the lapse rate tropopause calculated from each model’s piControl run as in Huang et al. (2016) for comparison to that study. The kernel-calculated

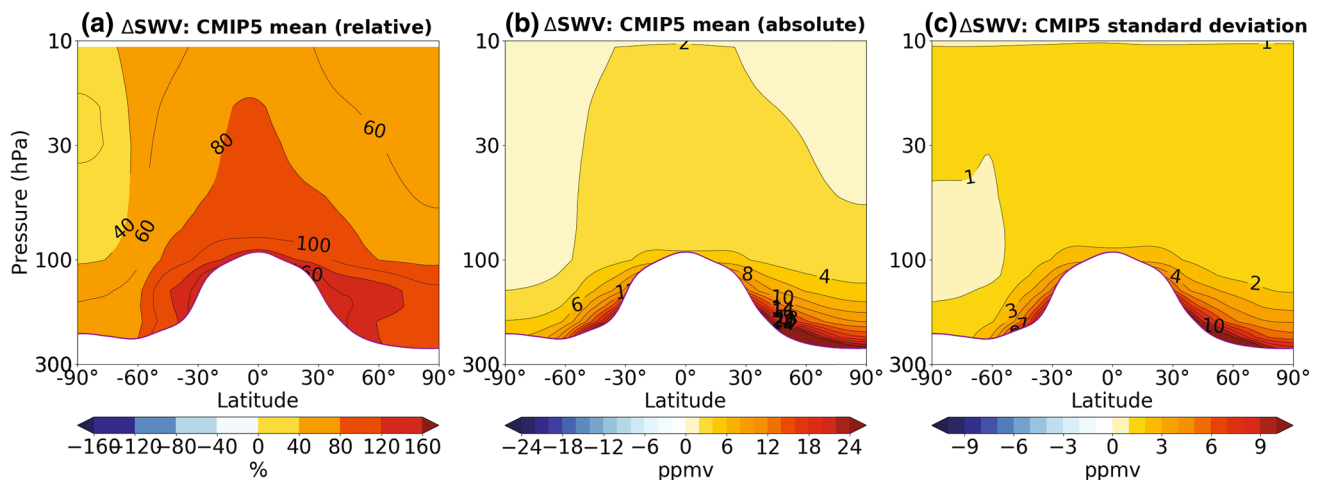


Fig. 1 The **a** relative (%) and **b** absolute (ppmv) zonal and climatological annual mean response of SWV to $4 \times \text{CO}_2$, averaged across the CMIP5 models. **c** The standard deviation in the SWV response across the CMIP5 models. Values below the PORT piControl tropopause are masked out

global mean values for the SWV feedback are included in Supplementary Table 1.

There are caveats to utilising CMIP5 model output from the abrupt $4 \times \text{CO}_2$ experiment to quantify the SWV feedback. The CMIP5 models generally have coarse vertical resolution within the TTL, which may limit the representation of processes (e.g. deep convection, the stratospheric circulation) that are important to simulating SWV amounts either via cold-point temperatures (Kim et al. 2013) or direct injection. It is conceivable that the strength of the contributing processes, and hence SWV amounts, do not scale linearly with increasing CO_2 concentrations, particularly to the large effects of CO_2 quadrupling. Indeed, non-linearities in the strength of climate feedbacks and the equilibrium climate sensitivity (ECS) in the magnitude of the forcing have previously been noted (e.g. Meraner et al. 2013; Vial et al. 2013). However, the aim of the present study is not to assess the models' ability to represent SWV nor to investigate non-linearities in a changing climate. Instead, we simply wish to quantify the SWV feedback strength in the CMIP abrupt $4 \times \text{CO}_2$ framework, within which the traditional set of feedbacks - as well as the ECS - are widely quantified (e.g. Gregory et al. 2004; Andrews et al. 2012; Vial et al. 2013).

3 Results

3.1 SWV response

Figures 1a, b show the response of SWV to $4 \times \text{CO}_2$ as relative (%) and absolute (ppmv) changes from the piControl for the CMIP5 multi-model mean; the respective responses in each individual model are shown in Figs. 2 and 3. The multi-model mean shows a moistening throughout the stratosphere;

averaging over the stratosphere gives a response of 3.0 ± 1.2 ppmv or $75 \pm 45\%$ (multi-model mean $\pm 1\sigma$).

A noticeable hemispheric asymmetry is evident in the response. The increase is smallest over Antarctica, with some models even showing a dehydration over this region. Larger increases are found in the Northern Hemisphere (NH) than in the Southern Hemisphere (SH), which might reflect greater increases in the NH in the strength of the stratospheric residual circulation or in cross tropopause isentropic mixing, potentially through intensified NH monsoon circulations (Dethof et al. 2000).

More importantly, we note a clear difference in the SWV response between the LMS and the overworld, also noted by Dessler et al. (2013). The multi-model mean, and nearly all models, show the largest SWV increases within the LMS (below 100 hPa, i.e. mainly in the extratropics). The LMS averaged response (6.0 ± 2.1 ppmv) is three times the overworld averaged response (2.1 ± 1.1 ppmv), and also larger on relative terms despite the larger SWV background in the LMS. Thus, based on the SWV response alone, the LMS might be expected to exert greater radiative effects than the overworld; this will be shown in Sect. 3.3.

While there are qualitative similarities in the SWV response between the models, the inter-model spread is large, with a standard deviation of 33% (LMS) and 50% (overworld) relative to the mean response (see also Fig. 1c). The CSIRO-Mk3-6-0 model stands out as having a particularly large response (see Figs. 2 and 3), which is conceivably due to its very low atmospheric vertical resolution (18 levels, with only one layer representing the tropical tropopause) (Gordon et al. 2002). We show in the next section that the multi-model spread of the SWV radiative perturbation, and its climate feedback, are related to the spread in the SWV response.

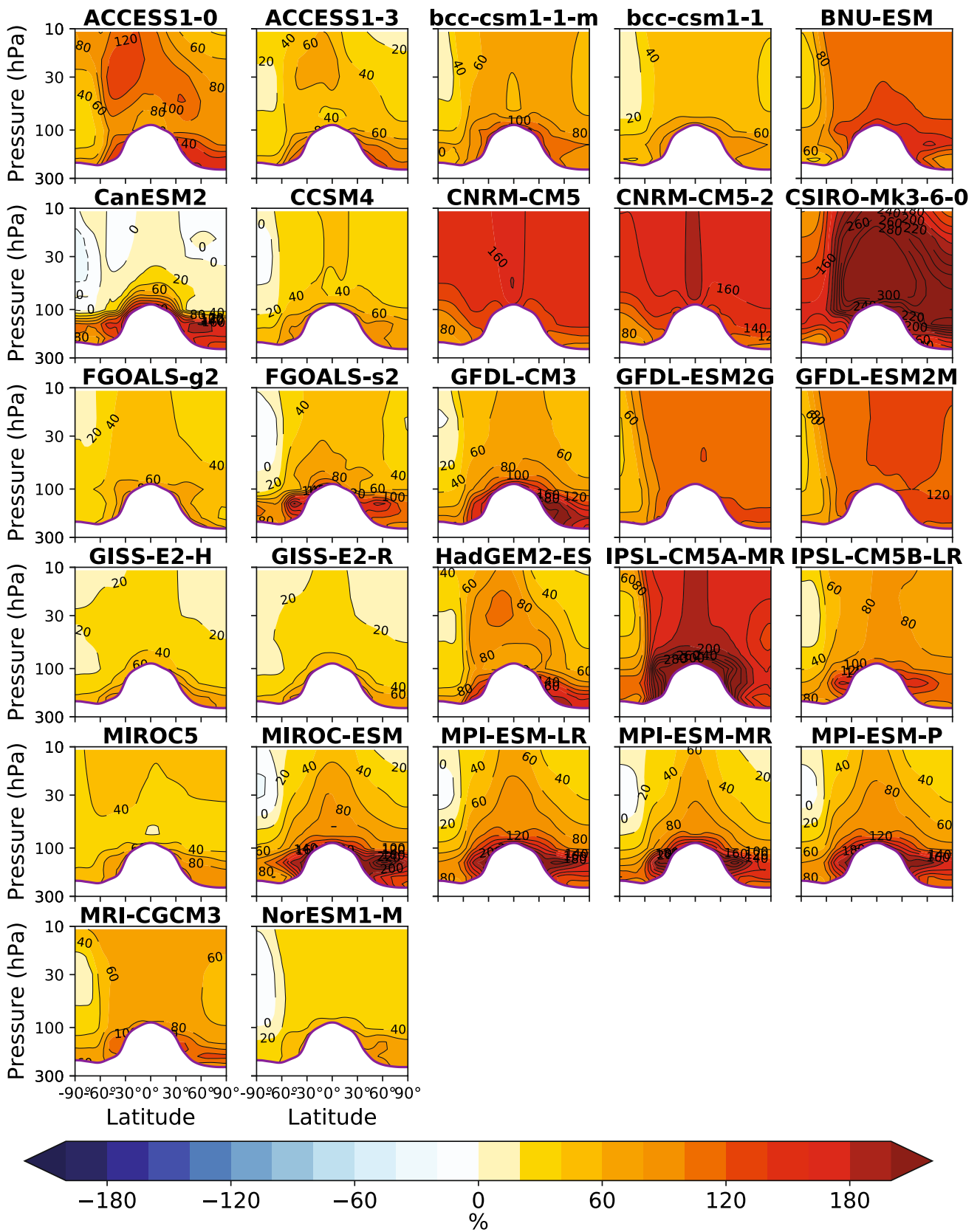


Fig. 2 The relative (%) response of SWV to $4 \times \text{CO}_2$ in individual CMIP5 models. Values below the PORT piControl tropopause are masked out

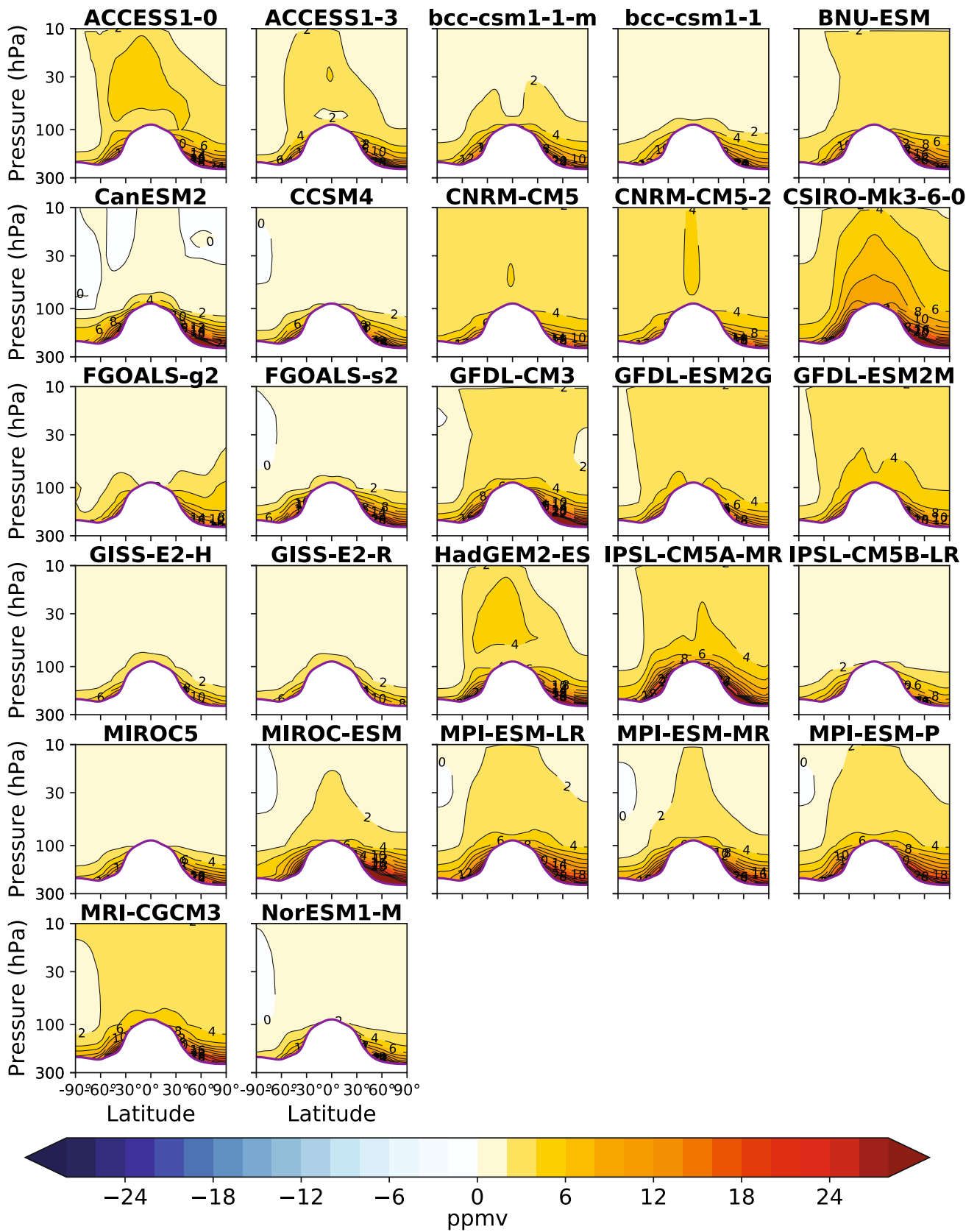


Fig. 3 The absolute (ppmv) response of SWV to $4\times\text{CO}_2$ in individual CMIP5 models. Values below the PORT piControl tropopause are masked out

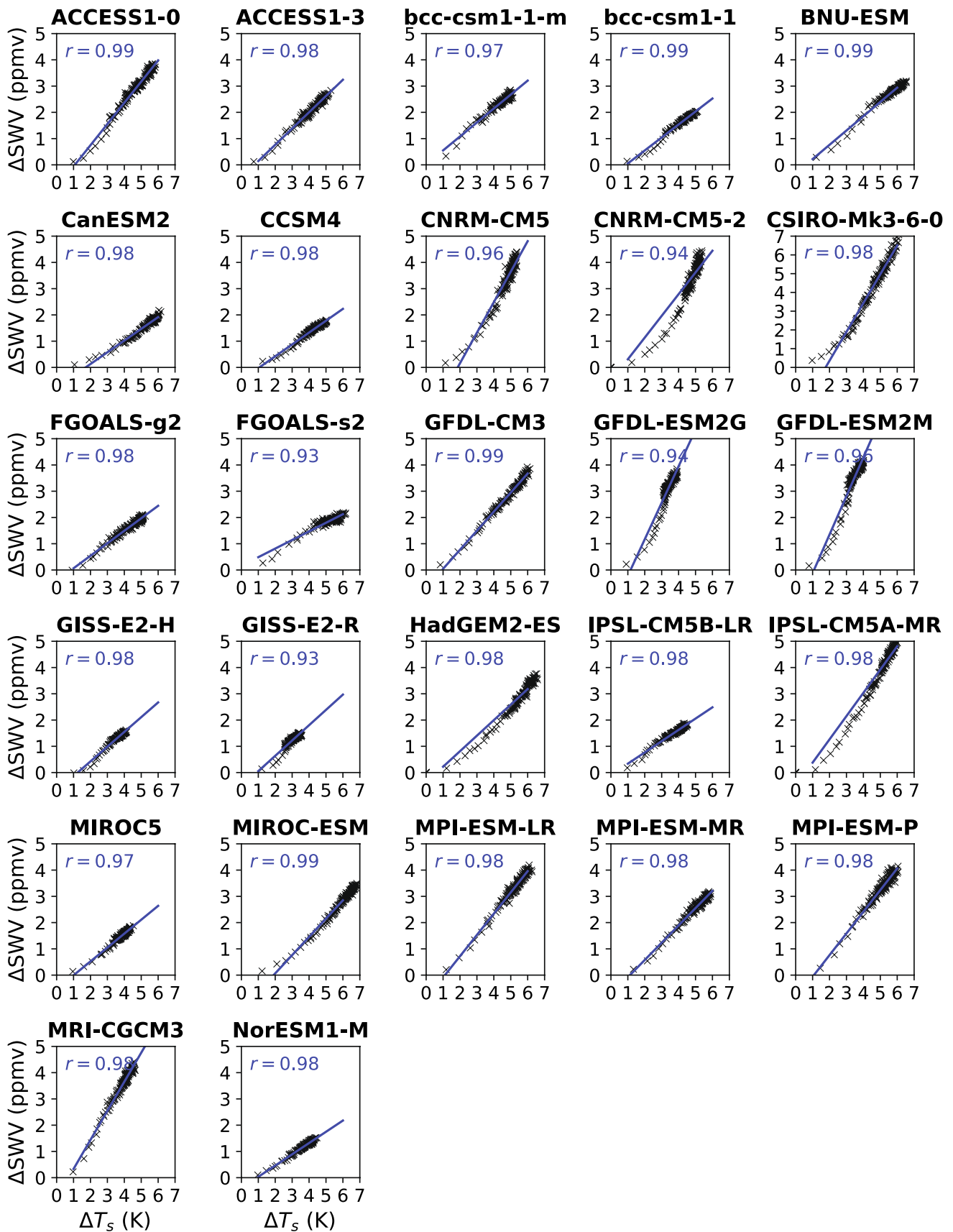


Fig. 4 Scatter plot showing the annual mean SWV response (averaged over the entire stratosphere; Δ SWV in ppmv) against ΔT_s (K) for the abrupt $4 \times \text{CO}_2$ simulation each model. The anomalies are with respect to the climatological annual mean of each model's piControl simulation. Note the larger y-axis scale for CSIRO-Mk3-6-0

3.2 Global mean SWV-induced radiative perturbation and climate feedback

We first show evidence that the long-term SWV response to increased CO_2 is likely to constitute a true climate feedback process, rather than a rapid adjustment contributing to CO_2 forcing. As mentioned in the Introduction, one method to demonstrate this is through the linear regression approach of Gregory et al. (2004), which would distinguish the part of the SWV radiative perturbation that is correlated to changing T_s (i.e. the climate feedback) from the part that is associated with rapid adjustment. However, such an exercise would require an excessive number of PRP calculations (one for each individual model year) and this is computationally not feasible⁴. Instead, here we simply show the SWV response itself (averaged over the entire stratosphere; Δ SWV) against ΔT_s for each model in Fig. 4 over the entire length of the abrupt $4 \times \text{CO}_2$ simulation (150 years). The fast SWV response (by the end of year 1) is only around 5% (up to 15% at most) of the response by the end of the simulation⁵. Rather, Δ SWV increases in close correlation with ΔT_s (linear correlation coefficients, r , range between 0.93 and 0.99). Assuming that the associated SWV radiative perturbation will behave the same way, we conclude that the SWV changes largely constitute a climate feedback mechanism.

In Figure 5a, it can be seen that net R_{adj} shows a strong linear relationship with Δ SWV across the CMIP5 ensemble of models. That is, we find a stronger radiative perturbation in models with a larger SWV response, which is unsurprising given the similar *pattern* of response across the models. The multi-model mean value of net R_{adj} at the tropopause is $0.89 \pm 0.27 \text{ Wm}^{-2}$, which is 30% smaller than net R_{ins} ($1.28 \pm 0.40 \text{ Wm}^{-2}$). At the ToA, the stratospheric adjustment has an even larger fractional impact, increasing the radiative perturbation by over a factor of six (see

Supplementary Table 1). This finding confirms many previous studies (Forster and Shine 1997; Solomon et al. 2010; Maycock and Shine 2012) that have shown the importance of the stratospheric adjustment for SWV's radiative effects, and have emphasized that it needs to be accounted for when assessing the magnitude of the associated climate feedback. Hereafter, we restrict our discussion to R_{adj} [at the tropopause, following Dessler et al. (2013)].

The net SWV climate feedback is calculated by normalizing net R_{adj} by ΔT_s for each model. This yields a multi-model mean SWV climate feedback of $0.17 \pm 0.05 \text{ Wm}^{-2} \text{ K}^{-1}$, with an inter-model range spanning $0.12\text{--}0.28 \text{ Wm}^{-2} \text{ K}^{-1}$. Taking into account the higher tropopause under $4 \times \text{CO}_2$ conditions lowers the feedback to $0.15 \pm 0.04 \text{ Wm}^{-2} \text{ K}^{-1}$ (range of $0.10\text{--}0.26 \text{ Wm}^{-2} \text{ K}^{-1}$; Supplementary Table 2). Interestingly, Fig. 5b demonstrates a linear correlation between Δ SWV and the associated climate feedback across the models. Only two GFDL models, which lie on the lower end of climate sensitivities (Table 1) but on the higher end of SWV responses (Fig. 5), are apparent outliers. The CSIRO-Mk3-6-0 model, which shows the largest SWV response, also shows the largest feedback, but nevertheless falls on the linear relationship. Removing these 3 models, and another high feedback model (IPSL-CM5A-MR), from the mean has little impact on the calculated feedback, decreasing it to $0.16 \pm 0.03 \text{ Wm}^{-2} \text{ K}^{-1}$. These results show that the inter-model spread in the SWV response is strongly related to the inter-model spread in its climate feedback, and the spread is large (1σ is around 20–30% of the multi-model mean) in both. Moreover, these results suggest that a model's long-term SWV response to increased CO_2 could be used as a proxy for the associated climate feedback.

Our calculated multi-model mean feedback - with a full range of between 0.10 to $0.28 \text{ Wm}^{-2} \text{ K}^{-1}$ - is consistent with (if slightly lower than) earlier estimates derived, using a similar method, with individual models by Dessler et al. (2013) ($0.29 \text{ Wm}^{-2} \text{ K}^{-1}$) and Stuber et al. (2001a) ($0.24 \text{ Wm}^{-2} \text{ K}^{-1}$; derived from the values in the final row of their Table 1), thereby broadly confirming their results. Here, we have also highlighted the large inter-model range in the SWV feedback present in the current generation of climate models. The very small value of the feedback found in Huang et al. (2016) ($0.02 \pm 0.01 \text{ Wm}^{-2} \text{ K}^{-1}$) can be attributed to the absence of the stratospheric temperature adjustment in their (instantaneous ToA) radiative kernel: we have been able to reproduce their small values both with the ToA R_{ins} calculations using PORT ($0.03 \pm 0.01 \text{ Wm}^{-2} \text{ K}^{-1}$) and with the ECHAM instantaneous ToA kernel ($0.02 \pm 0.01 \text{ Wm}^{-2} \text{ K}^{-1}$) (see Table 1 in Supplementary Information).

Finally, we note that in comparison to current estimates of tropospheric feedbacks, the SWV feedback calculated here is an order of magnitude smaller than the CMIP5 multi-model mean tropospheric water vapor feedback

⁴ Given the computational expense, the PRP procedure has been combined with the Gregory et al. (2004) linear regression approach to diagnose individual feedbacks in very few studies, such as Colman and McAvaney (2011), Meraner et al. (2013) and Colman (2015).

⁵ Technically, the fast SWV response should be determined at $\Delta T_s = 0$. The y-intercepts of the linear regression lines suggest a negative fast response for many of the models. An initial reduction in SWV could conceivably arise through CO_2 -induced cooling of the stratosphere and TTL. However, some degree of non-linearity is clearly evident for most models, such that the fast response might actually be zero or small positive.

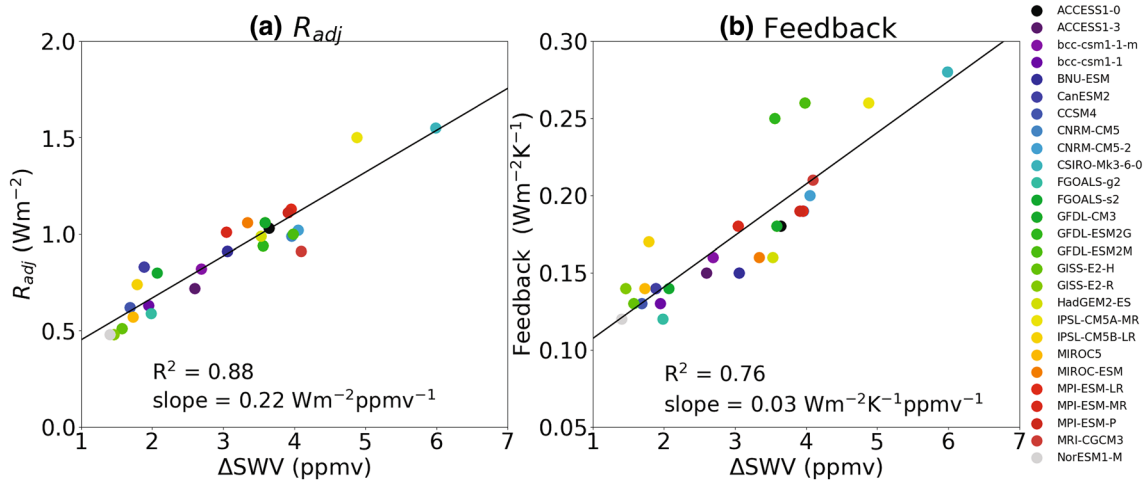
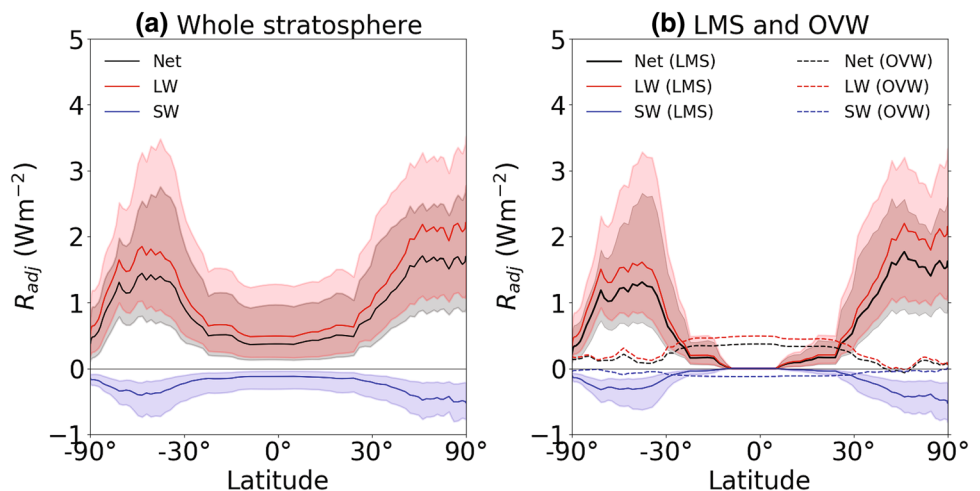


Fig. 5 Scatter plots showing **a** net R_{adj} (Wm^{-2}) measured at the tropopause under the piControl tropopause definition and **b** the corresponding climate feedback ($\text{Wm}^{-2} \text{K}^{-1}$) against the SWV response (ΔSWV , ppmv) to $4 \times \text{CO}_2$, using values in Table 1. Each point represents one model

Fig. 6 The latitudinal variations in R_{adj} (Wm^{-2}) measured at the tropopause under the piControl tropopause definition. The x -coordinate is in $\sin(\text{latitude})$ to show areal contributions to the global mean. **a** The net (black lines), LW (red lines) and SW (blue lines) R_{adj} due to SWV for the CMIP5 multi-model mean (solid lines) and the inter-model range (shading). **b** As in **a** but for the SWV response in the LMS only (solid lines) and in the overworld (dashed lines; calculated as the difference in R_{adj} between the whole stratosphere and the LMS)



[$1.6 \pm 0.3 \text{ Wm}^{-2} \text{ K}^{-1}$; Table 9.5 in Flato et al. (2013)]. However, it is of the same order of magnitude as the multi-model mean cloud feedback ($0.3 \pm 0.7 \text{ Wm}^{-2} \text{ K}^{-1}$, though we note its larger inter-model range) and surface albedo feedback ($0.3 \pm 0.1 \text{ Wm}^{-2} \text{ K}^{-1}$). We thus deem SWV changes an important climate feedback.

3.3 The role of the LMS

Having discussed the overall SWV response and climate feedback in the CMIP5 abrupt $4 \times \text{CO}_2$ simulations, we now focus on contributions from specific regions of the stratosphere. The LMS and stratospheric overworld have distinct controlling mechanisms (see Introduction) and responses to $4 \times \text{CO}_2$ (Fig. 1a, b). Therefore, we have separated their effects by performing a further set of radiative calculations

wherein SWV perturbations are imposed in the LMS only; as a reminder, most of this region is extratropical. Global mean results are shown in Supplementary Table 4.

Figure 6a shows the latitudinal contributions to R_{adj} (under the piControl tropopause definition). The net R_{adj} (LW+SW, black line) is dominated by the LW component (red line) and peaks in the midlatitudes of both hemispheres. Figure 6b highlights the LMS as the region of the largest SWV radiative perturbation (solid lines), characterized by two extratropical peaks, while the overworld response (dashed lines) makes a smaller contribution, characterized by a tropical peak. Indeed, we find that the LMS represents 77% of global mean R_{adj} (and hence, of the climate feedback) in the multi-model mean, with an inter-model range of ~60–95% (Supplementary Table 4). This result is an upper limit, as the relative contribution of the LMS will be smaller when accounting for the higher $4 \times \text{CO}_2$ tropopause height.

Nevertheless, our value is in good agreement with Dessler et al. (2013), who found a 66% contribution of the LMS in their single model study. The major role of the LMS can be explained by the greater underlying temperature sensitivity of this region (relative to the overworld) to a *uniform* SWV perturbation (Forster and Shine 2002; Maycock et al. 2011), combined with the largest SWV changes in terms of absorber mass from increased CO₂ occurring here (see Sect. 3.1). While most previous studies have delved into drivers of variability in tropical lower stratospheric SWV concentrations (Oman et al. 2008; Dessler et al. 2014; Hardiman et al. 2015; Smalley et al. 2017), our results add to the body of literature (Maycock et al. 2011; Dessler et al. 2013; Gilford et al. 2016; Huang et al. 2016) that motivates further efforts to understand drivers of *extratropical* lower stratospheric variability, given its importance for radiation and climate. Indeed, part of the extratropical variability could be linked to tropical variability through isentropic mixing (Gilford et al. 2016).

4 Discussion

Our study adds to the limited multi-model evidence in the literature on the importance of SWV as a climate feedback (Stuber et al. 2001a; Dessler et al. 2013). Dessler et al. (2013) employed a CCM and 21st century scenario in their study, in contrast to the CMIP5 abrupt 4 × CO₂ framework employed here. It is conceivable that the feedback calculated under 4 × CO₂ conditions is not representative of that occurring due to the smaller radiative forcing over the 21st century. In addition, CCMs—as opposed to the majority of models used here, which do not compute chemistry—might better simulate the SWV response to increasing CO₂ due to their (often) finer vertical resolution around the tropopause and representation of the complex dynamical and microphysical processes (Hardiman et al. 2015) that determine SWV amounts. The treatment of ozone under increased CO₂—prescribed as in most climate models versus interactive in CCMs—has also been shown to modify the SWV radiative perturbation and climate feedback, but the magnitude of the effect is strongly model dependent (Dietmüller et al. 2014; Nowack et al. 2015; Marsh et al. 2016). We note that the only three models in our CMIP5 ensemble which are CCMs (CNRM-CM5, CNRM-CM5-2 and GFDL-CM3) show no notable difference in their SWV feedback compared to the rest of the models (e.g. Table 1). We also find no significant difference in the feedback between models with high tops (above the stratopause) versus low tops in the global mean (0.18 ± 0.04 and $0.17 \pm 0.05 \text{ Wm}^{-2} \text{ K}^{-1}$ respectively under the piControl tropopause), nor any particular difference in the extratropics in contrast to Huang et al. (2016). Whether the SWV feedback is sensitive to the choice of model (CCMs

versus classical climate models) and magnitude of CO₂ forcing warrants future investigation. Despite the model differences, our value for the SWV climate feedback is broadly consistent with that found in Dessler et al. (2013) ($0.29 \text{ Wm}^{-2} \text{ K}^{-1}$) as well as Stuber et al. (2001a) ($0.24 \text{ Wm}^{-2} \text{ K}^{-1}$).

A few studies have quantified the separate stratospheric water vapor and/or temperature feedbacks (Chung and Soden 2015; Zhang and Huang 2014; Huang et al. 2016; Rieger et al. 2017). Chung and Soden (2015) and Huang et al. (2016) both find a negligible SWV feedback, which can be explained by the lack of the crucial stratospheric temperature adjustment considered as part of the feedback. Indeed, using PRP-like and radiative kernel techniques, we derive ToA instantaneous SWV feedback values of only $0.03 \pm 0.01 \text{ Wm}^{-2} \text{ K}^{-1}$ and $0.02 \pm 0.01 \text{ Wm}^{-2} \text{ K}^{-1}$, respectively. However, these previous studies also find a negligible stratospheric temperature feedback: this seems somewhat at odds with our results [and with those of Stuber et al. (2001a) and Dessler et al. (2013)], which show that the SWV feedback is mainly associated with stratospheric temperature changes. We speculate that factors besides SWV, such as the stratospheric circulation or clouds, might cancel the effects of SWV on the overall stratospheric temperature feedback; this too requires further investigation.

5 Conclusions

In this study, we have provided an estimate of the climate feedback of stratospheric water vapor (SWV) under the abrupt 4 × CO₂ scenario in 27 Coupled Model Intercomparison Project (CMIP5) models. The models robustly show a moistening of the stratosphere. The fast (<1 year) SWV response is only around 5% of the final response; instead, the transient SWV response is closely correlated with the slowly varying surface temperature response, supporting the role of SWV as a climate feedback mechanism. Imposing the SWV response in offline radiative calculations, broadly following a Partial Radiative Perturbation (PRP) approach, we find an associated global mean net stratosphere adjusted radiative perturbation of $0.89 \pm 0.27 \text{ W m}^{-2}$. The associated climate feedback is estimated to be $0.17 \pm 0.05 \text{ Wm}^{-2} \text{ K}^{-1}$ (ranging from 0.12 to $0.28 \text{ Wm}^{-2} \text{ K}^{-1}$ across the CMIP5 models). Taking into account the higher tropopause under 4xCO₂ conditions lowers the feedback to $0.15 \pm 0.04 \text{ Wm}^{-2} \text{ K}^{-1}$ (ranging from 0.10 to $0.26 \text{ Wm}^{-2} \text{ K}^{-1}$). As has long been recognized (Forster and Shine 1997; Solomon et al. 2010; Maycock and Shine 2012), the stratospheric temperature adjustment is a crucial part of the SWV radiative perturbation, and thus also of the associated climate feedback. We note that we have not assessed the effects of different model radiation schemes, which will be

an additional source of inter-model differences in the SWV feedback (Maycock and Shine 2012).

We have also found that the lowermost stratosphere (LMS), which is mainly located in the extratropics, is the key region for the feedback. The LMS response causes around three-quarters of the total SWV climate feedback in the multi-model mean (inter-model range of ~60–95%), which quantitatively agrees well with the single chemistry-climate model result (66%) of Dessler et al. (2013). While water vapor variability in the tropical tropopause layer (TTL) has been the subject of much attention (Oman et al. 2008; Dessler et al. 2014; Smalley et al. 2017), our results underscore the need for future studies to focus also on the extratropical LMS, e.g. on the importance of transport from the TTL itself (Gilford et al. 2016) versus transport across the tropopause (Stenke et al. 2008). The LMS—in addition to its importance for radiation and climate—might also be a critical region for determining the dynamical impacts of SWV (Tandon et al. 2011).

Finally, we wish to emphasize that although the SWV climate feedback calculated here is small compared to global mean estimates of the tropospheric water vapor feedback from the CMIP5 models, it is of the same order of magnitude as the multi-model mean surface albedo feedback ($0.3 \pm 0.1 \text{ Wm}^{-2} \text{ K}^{-1}$) and the cloud feedback ($0.3 \pm 0.7 \text{ Wm}^{-2} \text{ K}^{-1}$) [see Table 9.5 in Flato et al. (2013)], though we note the large inter-model range on the latter. As SWV represents an individual physical entity (controlled, at least in part, by essentially different mechanisms than tropospheric water vapor), we conclude that the SWV feedback is of sufficiently large amplitude to deserve dedicated attention. Model-to-model variations, as reported in the present paper, and full understanding of the underlying physical mechanisms need further investigation.

Acknowledgements This work was funded, in part, by grants from the US National Science Foundation (NSF) to Columbia University. The authors would like to thank Andrew Dessler, Yi Huang and an anonymous reviewer for helpful comments on this work. We would like to acknowledge high-performance computing support from Yellowstone (ark:/85065/d7wd3xhc) provided by NCAR's Computational and Information Systems Laboratory, sponsored by the National Science Foundation. We acknowledge the World Climate Research Programme's Working Group on Coupled Modelling, which is responsible for CMIP, and we thank the climate modeling groups for producing and making available their model output. For CMIP the U.S. Department of Energy's Program for Climate Model Diagnosis and Intercomparison provides coordinating support and led development of software infrastructure in partnership with the Global Organization for Earth System Science Portals.

Appendix

Two calculations are performed for each SWV perturbation to give the associated instantaneous (R_{ins}) and stratosphere-adjusted (R_{adj}) radiative perturbations. Here we describe

the calculation of R_{adj} under the Fixed Dynamical Heating (FDH) approximation (Ramanathan and Dickinson 1979; Fels et al. 1980; Forster et al. 1997; Stuber et al. 2001b); further details of its implementation in PORT can be found in Conley et al. (2013).

In every grid cell, the temperature tendency that results from a net heating rate is the sum of radiative (Q_{rad}) and dynamical (Q_{dyn}) heating rates, which are functions of temperature (T) and composition (C). In an unperturbed steady-state, the temperature tendency is equal to zero:

$$dT/dt = Q_{rad}(T, C) + Q_{dyn}(T, C) = 0 \quad (1)$$

A perturbation to the composition of the stratosphere (in our case, a change in SWV) can change the radiative heating rate to result in a non-zero temperature tendency. Under the FDH approximation, the dynamical heating rate is assumed to remain at unperturbed values, leading to a purely radiative equation:

$$dT/dt = Q_{rad}(T, C') + Q_{dyn}(T, C) = Q_{rad}(T, C') - Q_{rad}(T, C) \neq 0 \quad (2)$$

Stratospheric temperatures are iteratively adjusted in the above equation with a timestep of 30 min, while tropospheric and surface temperatures are held fixed, to reach another steady-state:

$$Q_{rad}(T', C') - Q_{rad}(T, C) = 0 \quad (3)$$

The model is run for 5 years; the first year is discarded to allow the stratosphere to reach steady state and results are averages over the following 4 years. $T' - T$ is the overall stratospheric temperature adjustment. R_{adj} is the vertical net radiative flux (downwards = positive) after stratospheric adjustment, here, measured at the tropopause and ToA, which should be equal at steady state. We find that defining the tropopause on a timestep-by-timestep basis leads to some instability in the calculation as the adjustment domain changes, as found by Stuber et al. (2001b), causing a difference between R_{adj} measured at the tropopause and ToA. Instead, we define a monthly varying tropopause that gives enough stability (tropopause and ToA values differ by at most 2%; e.g. compare Table 1 and Supplementary Table 1) as well as a seasonal variation to the calculation.

References

- Andrews T, Gregory JM, Webb MJ, Taylor KE (2012) Forcing, feedbacks and climate sensitivity in CMIP5 coupled atmosphere-ocean climate models. *Geophys Res Lett* 39(9):L09712
- Block K, Mauritsen T (2013) Forcing and feedback in the MPI-ESM-LR coupled model under abruptly quadrupled CO₂. *J Adv Model Earth Syst* 5(4):676–691
- Bony S, Colman R, Kattsov VM, Allan RP, Bretherton CS, Dufresne JL, Hall A, Hallegatte S, Holland MM, Ingram W et al (2006)

- How well do we understand and evaluate climate change feedback processes? *J Clim* 19(15):3445–3482
- Chung ES, Soden BJ (2015) An assessment of direct radiative forcing, radiative adjustments, and radiative feedbacks in coupled ocean-atmosphere models. *J Clim* 28(10):4152–4170
- Colman R (2015) Climate radiative feedbacks and adjustments at the Earth's surface. *J Geophys Res Atmos* 120(8):3173–3182
- Colman R, McAvaney B (1997) A study of general circulation model climate feedbacks determined from perturbed sea surface temperature experiments. *J Geophys Res Atmos* 102(D16):19,383–19,402
- Colman R, McAvaney B (2011) On tropospheric adjustment to forcing and climate feedbacks. *Clim Dyn* 36(9–10):1649
- Conley A, Lamarque JF, Vitt F, Collins W, Kiehl J (2013) PORT, a CESM tool for the diagnosis of radiative forcing. *Geosci Model Dev* 6(2):469–476
- Dessler A, Schoeberl M, Wang T, Davis S, Rosenlof K (2013) Stratospheric water vapor feedback. *Proc Natl Acad Sci USA* 110(45):18,087–18,091
- Dessler A, Schoeberl M, Wang T, Davis S, Rosenlof K, Vernier JP (2014) Variations of stratospheric water vapor over the past three decades. *J Geophys Res Atmos* 119(22):12–588
- Dessler A, Ye H, Wang T, Schoeberl M, Oman L, Douglass A, Butler A, Rosenlof K, Davis S, Portmann R (2016) Transport of ice into the stratosphere and the humidification of the stratosphere over the 21st century. *Geophys Res Lett* 43(5):2323–2329
- Dethof A, O'Neill A, Slingo J, Berrisford P (2000) Quantification of isentropic water-vapour transport into the lower stratosphere. *Q J R Meteorol Soc* 126(566):1771–1788
- Dietmüller S, Ponater M, Sausen R (2014) Interactive ozone induces a negative feedback in CO₂-driven climate change simulations. *J Geophys Res Atmos* 119(4):1796–1805
- Fels S, Mahlman J, Schwarzkopf M, Sinclair R (1980) Stratospheric sensitivity to perturbations in ozone and carbon dioxide: radiative and dynamical response. *J Atmos Sci* 37(10):2265–2297
- Flato G, Marotzke J, Abiodun B, Braconnot P, Chou SC, Collins W, Cox P, Driouech F, Emori S, Eyring V et al (2013) Evaluation of climate models. In: Stocker T, Qin D, Plattner GK, Tignor M, Allen S, Boschung J, Nauels A, Xia Y, Bex V, Midgley P (eds) *Climate Change 2013: The Physical Science Basis*. Contribution of Working Group I to the Fifth Assessment Report of the Intergovernmental Panel on Climate Change. Cambridge University Press, Cambridge
- Forster PMdF, Shine KP (1997) Radiative forcing and temperature trends from stratospheric ozone changes. *J Geophys Res Atmos* 102(D9):10,841–10,855
- Forster PMdF, Shine K (2002) Assessing the climate impact of trends in stratospheric water vapor. *Geophys Res Lett* 29(6):10–1
- Forster PMF, Freckleton RS, Shine KP (1997) On aspects of the concept of radiative forcing. *Clim Dyn* 13(7):547–560. <https://doi.org/10.1007/s003820050182>
- Fueglistaler S, Haynes P (2005) Control of interannual and longer-term variability of stratospheric water vapor. *J Geophys Res Atmos* 110(D24):D24108
- Gottelman A, Birner T, Eyring V, Akiyoshi H, Bekki S, Brühl C, Dameris M, Kinnison D, Lefèvre F, Lott F et al (2009) The tropical tropopause layer 1960–2100. *Atmos Chem Phys* 9(5):1621–1637
- Gottelman A, Hegglin MI, Son SW, Kim J, Fujiwara M, Birner T, Kremser S, Rex M, Añel J, Akiyoshi H et al (2010) Multimodel assessment of the upper troposphere and lower stratosphere: tropics and global trends. *J Geophys Res Atmos* 115(D3):D00M08
- Gilford DM, Solomon S, Portmann RW (2016) Radiative impacts of the 2011 abrupt drops in water vapor and ozone in the tropical tropopause layer. *J Clim* 29(2):595–612
- Gordon HB, Rotstayn LD, McGregor JL, Dix MR, Kowalczyk EA, O'Farrell SP, Waterman LJ, Hirst AC, Wilson SG, Collier MA, Watterson IG, Elliott TI (2002) The CSIRO Mk3 climate system model. Technical Paper 60, CSIRO Atmospheric Research. <http://www.cmar.csiro.au/e-print/open/gordon2002a.pdf>
- Gregory J, Ingram W, Palmer M, Jones G, Stott P, Thorpe R, Lowe J, Johns T, Williams K (2004) A new method for diagnosing radiative forcing and climate sensitivity. *Geophys Res Lett* 31(3):L03205
- Hardiman SC, Boutle IA, Bushell AC, Butchart N, Cullen MJ, Field PR, Furtado K, Manners JC, Milton SF, Morcrette C et al (2015) Processes controlling tropical tropopause temperature and stratospheric water vapor in climate models. *J Clim* 28(16):6516–6535
- Hegglin M, Plummer D, Shepherd T, Scinocca J, Anderson J, Froidevaux L, Funke B, Hurst D, Rozanov A, Urban J et al (2014) Vertical structure of stratospheric water vapour trends derived from merged satellite data. *Nat Geosci* 7(10):768
- Holton JR, Gettelman A (2001) Horizontal transport and the dehydration of the stratosphere. *Geophys Res Lett* 28(14):2799–2802
- Huang Y (2013) On the longwave climate feedbacks. *J Clim* 26(19):7603–7610. <https://doi.org/10.1175/JCLI-D-13-00025.1>
- Huang Y, Zhang M, Xia Y, Hu Y, Son SW (2016) Is there a stratospheric radiative feedback in global warming simulations? *Clim Dyn* 46(1–2):177–186
- Kim J, Grise KM, Son SW (2013) Thermal characteristics of the cold-point tropopause region in CMIP5 models. *J Geophys Res Atmos* 118(16):8827–8841
- Klocke D, Quaas J, Stevens B (2013) Assessment of different metrics for physical climate feedbacks. *Clim Dyn* 41(5–6):1173–1185
- Liu R, Su H, Liou KN, Jiang JH, Gu Y, Liu SC, Shiu CJ (2018) An assessment of tropospheric water vapor feedback using radiative kernels. *J Geophys Res Atmos* 123(3):1499–1509
- Marsh DR, Lamarque JF, Conley AJ, Polvani LM (2016) Stratospheric ozone chemistry feedbacks are not critical for the determination of climate sensitivity in CESM1 (WACCM). *Geophys Res Lett* 43(8):3928–3934
- Maycock A, Shine K (2012) Stratospheric water vapor and climate: Sensitivity to the representation in radiation codes. *J Geophys Res Atmos* 117(D13):D13102
- Maycock AC, Shine KP, Joshi MM (2011) The temperature response to stratospheric water vapour changes. *Q J R Meteorol Soc* 137(657):1070–1082
- Meraner K, Mauritsen T, Voigt A (2013) Robust increase in equilibrium climate sensitivity under global warming. *Geophys Res Lett* 40(22):5944–5948
- Nowack PJ, Abraham NL, Maycock AC, Braesicke P, Gregory JM, Joshi MM, Osprey A, Pyle JA (2015) A large ozone-circulation feedback and its implications for global warming assessments. *Nat Clim Change* 5(1):41
- Oman L, Waugh DW, Pawson S, Stolarski RS, Nielsen JE (2008) Understanding the changes of stratospheric water vapor in coupled chemistry–climate model simulations. *J Atmos Sci* 65(10):3278–3291
- Pan LL, Hintsa EJ, Stone EM, Weinstock EM, Randel WJ (2000) The seasonal cycle of water vapor and saturation vapor mixing ratio in the extratropical lowermost stratosphere. *J Geophys Res Atmos* 105(D21):26,519–26,530
- Previdi M (2010) Radiative feedbacks on global precipitation. *Environ Res Lett* 5(2):025211
- Previdi M, Liepert BG (2012) The vertical distribution of climate forcings and feedbacks from the surface to top of atmosphere. *Clim Dyn* 39(3–4):941–951
- Ramanathan V, Dickinson RE (1979) The role of stratospheric ozone in the zonal and seasonal radiative energy balance of the earth-troposphere system. *J Atmos Sci* 36(6):1084–1104. [https://doi.org/10.1175/1520-0469\(1979\)036<1084:TROSOL>2.0.CO;2](https://doi.org/10.1175/1520-0469(1979)036<1084:TROSOL>2.0.CO;2)
- Rieger VS, Dietmüller S, Ponater M (2017) Can feedback analysis be used to uncover the physical origin of climate sensitivity and efficacy differences? *Clim Dyn* 49(7–8):2831–2844

- Sanderson BM, Shell KM, Ingram W (2010) Climate feedbacks determined using radiative kernels in a multi-thousand member ensemble of AOGCMs. *Clim Dyn* 35(7–8):1219–1236
- Shell KM, Kiehl JT, Shields CA (2008) Using the radiative kernel technique to calculate climate feedbacks in NCAR's community atmospheric model. *J Clim* 21(10):2269–2282
- Smalley KM, Dessler AE, Bekki S, Deushi M, Marchand M, Morgenstern O, Plummer DA, Shibata K, Yamashita Y, Zeng G (2017) Contribution of different processes to changes in tropical lower-stratospheric water vapor in chemistry–climate models. *Atmos Chem Phys* 17(13):8031–8044
- Soden BJ, Held IM (2006) An assessment of climate feedbacks in coupled ocean–atmosphere models. *J Clim* 19(14):3354–3360
- Soden BJ, Held IM, Colman R, Shell KM, Kiehl JT, Shields CA (2008) Quantifying climate feedbacks using radiative kernels. *J Clim* 21(14):3504–3520
- Solomon S, Rosenlof KH, Portmann RW, Daniel JS, Davis SM, Sanford TJ, Plattner GK (2010) Contributions of stratospheric water vapor to decadal changes in the rate of global warming. *Science* 327(5970):1219–1223
- Stenke A, Grewe V, Ponater M (2008) Lagrangian transport of water vapor and cloud water in the ECHAM4 GCM and its impact on the cold bias. *Clim Dyn* 31(5):491–506
- Stuber N, Ponater M, Sausen R (2001a) Is the climate sensitivity to ozone perturbations enhanced by stratospheric water vapor feedback? *Geophys Res Lett* 28(15):2887–2890
- Stuber N, Sausen R, Ponater M (2001b) Stratosphere adjusted radiative forcing calculations in a comprehensive climate model. *Theor Appl Climatol* 68(3):125–135. <https://doi.org/10.1007/s007040170041>
- Sun Y, Huang Y (2015) An examination of convective moistening of the lower stratosphere using satellite data. *Earth Space Sci* 2(7):320–330
- Tandon NF, Polvani LM, Davis SM (2011) The response of the tropospheric circulation to water vapor-like forcings in the stratosphere. *J Clim* 24(21):5713–5720
- Vial J, Dufresne JL, Bony S (2013) On the interpretation of inter-model spread in CMIP5 climate sensitivity estimates. *Clim Dyn* 41(11–12):3339–3362
- Wetherald R, Manabe S (1988) Cloud feedback processes in a general circulation model. *J Atmos Sci* 45(8):1397–1416
- WMO (1957) Meteorology—a three-dimensional science: Second session of the commission for aerology. *WMO Bull* 4(4):134–138
- Zhang M, Huang Y (2014) Radiative forcing of quadrupling CO_2 . *J Clim* 27(7):2496–2508. <https://doi.org/10.1175/JCLI-D-13-00535.1>

Publisher's Note Springer Nature remains neutral with regard to jurisdictional claims in published maps and institutional affiliations.